

# Design and Fabrication of Compliant Micromechanisms and Structures with Negative Poisson's Ratio

Ulrik Darling Larsen, Ole Sigmund, and Siebe Bouwstra

**Abstract**— This paper describes a new way to design and fabricate compliant micromechanisms and material structures with negative Poisson's ratio (NPR). The design of compliant mechanisms and material structures is accomplished in an automated way using a numerical topology optimization method. The procedure allows the user to specify the elastic properties of materials or the mechanical advantages (MA's) or geometrical advantages (GA's) of compliant mechanisms and returns the optimal structures. The topologies obtained by the numerical procedure require practically no interaction by the engineer before they can be transferred to the fabrication unit. Fabrication is carried out by patterning a sputtered silicon on a plasma-enhanced chemical vapor deposition (PECVD) glass with a laser micromachining setup. Subsequently, the structures are etched into the underlying PECVD glass, and the glass is underetched, all in one two-step reactive ion etching (RIE) process. The components are tested using a probe placed on an  $x$ - $y$  stage. This fast prototyping allows newly developed topologies to be fabricated and tested within the same day. [188]

**Index Terms**— Compliant micromechanism, fast prototyping, negative Poisson's ratio.

## I. INTRODUCTION

MICROMECHANICAL devices have many promising areas of application. Some of the main areas are tools for microfabrication and nanofabrication, microsurgery, and nanoprobe analysis systems. In nanofabrication, the manipulation of small objects on a surface by microhandling mechanisms, such as a microgripper [1] and positioning microrobotic devices [2], are steps forward toward higher functionality levels and higher flexibility. In microsurgery, where accuracy is needed in microscopic and very sensitive operations, the micromechanisms may provide very precise tweezers and knives, etc. In microanalysis and nanoanalysis systems, the micromechanisms can be used as positioning tools or for precision probing of a surface [3], whereas microtweezers can be used to hold the specimens [4].

While design tools for the electronic part of microelectromechanical systems (MEMS) are very well developed, problems such as methodical design of the mechanical parts, packaging,

and fabrication methods for MEMS still have to be solved. Here, we shall concentrate on design and fabrication of the mechanical parts. Because of the small dimensions, it is difficult to use ideal hinges, bearings, and rigid bodies, as seen in design of normal multibody systems (e.g., Erdman and Sandor [5]) for the design of MEMS. Friction and wear would cause the hinges to break down after a few operation cycles. Therefore, micromechanisms should be designed as compliant or flexible-link mechanisms. Compliant mechanisms also have the advantage that they can be built in one piece, which lowers the number of fabrication steps.

Fabrication of microstructures can be done using silicon-surface micromachining in thin-film materials. Currently, two-dimensional (2-D) fabrication procedures are well developed, but effort is devoted to the development of fabrication methods for two-and-a-half [6] and fully three-dimensional (3-D) micromechanisms [7]. This paper will only consider 2-D structures. The micromachining process should be compatible with general micromachining processes to facilitate the implementation with interface electronics and actuators. Furthermore, film thicknesses of more than  $5\text{ }\mu\text{m}$  are preferred to prevent buckling and warping of the structures during testing. These demands can be met by employing low-stress plasma-enhanced chemical vapor deposition (PECVD) glass. In this paper, the structures will be operated by external probes. On-chip integrated actuation would, in principle, be possible using, for example, thermal bimorph actuators [8]. In the case of electrically conductive structures, electrostatic comb drives can be applied.

## II. METHODOLOGICAL DESIGN OF COMPLIANT MECHANISMS

Design of compliant mechanisms is often accomplished by trial and error methods. However, Howell and Midha [9] suggest a method to design compliant mechanisms by modifications of a rigid body model. Ananthasuresh *et al.* [10] use topology optimization methods to find the compliant mechanism topology, which, in an optimal way, can perform a given manipulation task, and Sigmund [11] uses a truss model and topology optimization techniques to design simple grabbing mechanisms. Topology optimization is typically used as a design tool when high performance and low weight of a mechanical structure is required, which is often the case in the aerospace and automotive industries. This field has gained much popularity since Bendsøe and Kikuchi [12]

Manuscript received December 5, 1995; revised October 1, 1996. Subject Editor, D.-I. D. Cho. This work was supported by Denmark's Technical Research Council (Programme of Research on Computer-Aided Design).

U. D. Larsen and S. Bouwstra are with Mikroelektronik Centret (MIC), Technical University of Denmark, DK-2800 Lyngby, Denmark.

O. Sigmund is with the Department of Solid Mechanics, Technical University of Denmark, DK-2800 Lyngby, Denmark.

Publisher Item Identifier S 1057-7157(97)02119-7.

introduced a topology optimization method using homogenization methods. For an overview of the field, the reader is referred to Bendsøe [13] and the references therein. The method presented here is an improvement of the methods presented in [11] and [12] and allows the user to specify the mechanical advantages (MA's) or the geometrical advantages (GA's) of the compliant mechanisms. The topologies obtained require only little interpretation by the engineer before they can be transferred to the fabrication unit. For design of compliant mechanisms in this paper, the topology optimization problem is defined as follows. *Distribute a given amount of material within a design domain for a prescribed MA or GA and such that the mechanical efficiency is maximized.* The optimization problem is formulated as minimization of least-squares errors in obtaining the prescribed elastic behavior and is solved using a sequential linear programming (SLP) method.

#### A. Computational Method for Compliant Mechanisms

The main difference between rigid body mechanisms and compliant mechanisms is that energy is no longer conserved between the input and output point because of energy storage in the flexible parts of the latter. This implies that the GA is not equal to the inverse of the MA when we are considering compliant mechanisms. In other words, defining GA as output displacement divided by input displacement and MA as output force divided by input force,  $MA \cdot GA$  will be equal to one for rigid body mechanisms with ideal hinges, whereas  $MA \cdot GA$  will always be less than one for compliant mechanisms. One of the goals in compliant mechanism design is to get  $MA \cdot GA$  as close to one as possible—in that way, a high mechanical efficiency of the compliant device is ensured. Typically, the user wants a mechanism with some specific GA or MA  $GA^*$  or  $MA^*$ . There will also typically be some constraint on the amount of material that can be used for the structure. By choosing an upper limit  $V^*$  on the amount of material that can be distributed in the design domain, it is indirectly possible to control widths of beams in the designs.

The optimization problem can now be defined as follows. *Distribute a given amount of material within the design domain such that the error in obtaining the prescribed values of GA and MA are minimized.* The optimization problem can be written as

$$\begin{aligned} &\text{Minimize} \quad \Phi = \frac{(MA - MA^*)^2}{(MA^*)^2} + \frac{(GA - GA^*)^2}{(GA^*)^2} \\ &\text{subject to} \quad \sum_{e=1}^N \rho^e v^e \leq V^* \\ &\text{and} \quad 0 < \rho_{\min} \leq \rho^e \leq 1, \quad e = 1, \dots, N \end{aligned} \quad (1)$$

where  $N$  is the number of elements or design variables,  $\rho^e$  is the density of material in element  $e$  (design variable  $e$ ),  $\rho_{\min}$  is the lower side constraint on the design variables (for computational reasons), and  $v^e$  is the volume of element  $e$ . Typically, the algorithm requires several hundred iterations to converge, each iteration step requiring a finite-element analysis with two load cases [solving (1)], a simple analytical sensitivity analysis, and a design update using the Simplex algorithm. For more details on the computational algorithms

and methods, the reader is referred to the general literature on topology optimization (e.g., Bendsøe [13]).

#### B. Compliant Mechanism Design Examples

Fig. 1 shows the design domains and input and output load cases for five considered compliant mechanism design problems. The rectangular design domains are discretized by typically 3000 quadrilateral finite elements, where the density of material in each element represents one design variable. The resulting designs are shown in Fig. 2. By using penalization of gray areas in the design algorithm, the amount of gray areas is minimized, but, still, their appearance cannot be fully eliminated. The five mechanisms can be characterized as follows. Mechanism *a* is a force inverter that converts a horizontal input force to a force in the opposite direction at the output point. The MA's or GA's can be prescribed such that force or displacement amplification can be achieved. Fig. 2(a1) and (a2) shows a 1:1 and 4:1 force inverter, respectively. The mechanism in Fig. 2(a2) can also be seen as a displacement amplifier: an input displacement (black arrow) is converted to a four-times-bigger output displacement in the opposite direction. It should be noted that the design procedure only considers linear displacements, and, therefore, the GA's only hold for small input displacements. Fig. 2(b1) and 2(b2) shows the resulting designs for a cleaving mechanism (this design example was used in [10]). There are two input forces that should be converted into a compressive or tensile force at the output piston [which is prescribed to be solid, as seen in Fig. 1(b)]. Mechanisms *c* and *d* represent the design of gripping mechanisms. For grippers *c1* and *c2*, the output points are the outer points of the jaws, which are specified to close and open, subject to the horizontal input force, respectively. For grippers *d1* and *d2*, the jaws are specified to move in parallel. This was done by specifying two separate output load cases, and the design problem was therefore extended to include two prescribed GA's and two prescribed MA's. Finally, mechanism *e* represents the design of a micropositioning device. Given a design domain and two input actuators, the problem is to find the mechanism topology that can make the output point independently controllable in the vertical and horizontal directions, respectively. Fig. 2(e1) shows a design, where a horizontal input force (middle left edge) results in a horizontal movement of the output point, and a vertical input force (middle lower side) results in a vertical movement of the output point. If we want to use comb drives as actuators, we can only get attracting input forces. Fortunately, the design method is able to produce the micropositioning device seen in Fig. 2(e2); this mechanism has the opposite output behavior compared to *e1*. All these mechanisms can also be used in the opposite direction, where a force or displacement at the output gives an associated force or displacement at the input.

### III. DESIGN OF STRUCTURES WITH NPR

The existence of materials with NPR's or, in other words, the existence of materials that expand transversely subject to an applied tensile load has been questioned by researchers and

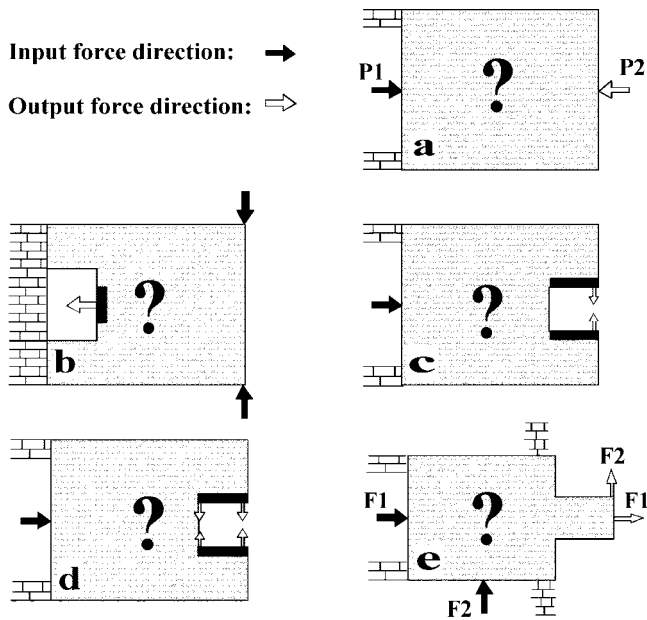


Fig. 1. Design domains and input and output load cases for five compliant mechanisms. The gray areas define the design domains, whereas white and black areas define areas that are specified to be void or to consist of solid material, respectively. Black arrows denote point and direction of the input force, and white arrows denote points and directions of the prescribed output forces or displacements. Numbers denote the magnitude of the forces.

engineers for a long time. However, thermodynamics allows the Poisson's ratio of an isotropic material to approach  $-1$ . Among other applications (see, e.g., Lakes [9]), materials with NPR can advantageously be used in the design of hydrophones [14] and other sensors. One reason is that the low-bulk modulus of these materials makes them more sensitive to hydrostatic pressure. As the bulk modulus of an isotropic material is defined as  $K = E/(3(1 - 2\nu))$ , where  $E$  is Young's modulus and  $\nu$  is Poisson's ratio, the sensitivity to hydrostatic pressure is increased by almost one order of magnitude for a Poisson's ratio  $-1$  material compared to a material with an ordinary Poisson's ratio  $0.3$ . A theoretical material microstructure with Poisson's ratio  $-1$  was first reported by Almgren [15]. A practical material with NPR was first developed by Lakes [16], who treated an open-walled foam material with heat and pressure to obtain the NPR effect. Lake's foams have average cell sizes down to  $0.3$  mm and Poisson's ratios down to  $-0.8$ . In Sigmund [11], [17], [18], a numerically based method is used to design materials with any thermodynamically admissible elastic properties. In this paper, we will show that it is possible to design and manufacture microstructures with NPR's and cell sizes down to  $50$  m using topology optimization. These microstructures are referred to as NPR materials and can be fabricated by utilizing silicon surface micromachining techniques.

It might be objected that the NPR materials produced in this work are structures rather than materials. However, knowing that every material has a structure if one looks at it at a sufficiently small scale, the distinction between "materials" and "structures" is blurred. Defining materials as repeated structures that cannot be seen by the naked eye, the negative Poisson's structures produced in this paper are

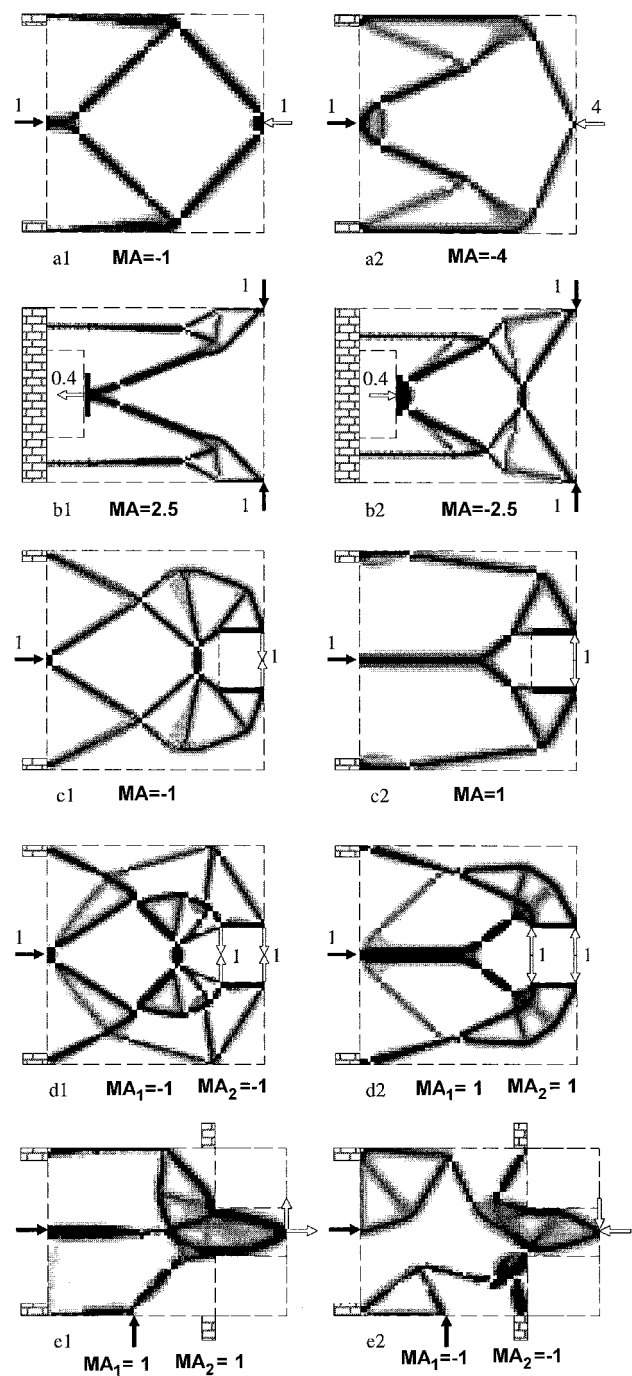


Fig. 2. Ten optimized compliant micromechanisms. White colors indicate void areas, black colors indicate solid areas, and gray areas indicate areas of medium density. Numbers denote the size of the forces.

materials indeed, and they are comparable to the naturally existing material cork (zero Poisson's ratio), which has a microstructure on the same length scale.

For the design of NPR materials, we will consider periodic microstructures, where the smallest repetitive unit, called the base cell, will be the design domain, and the design goal is to minimize the error in obtaining the prescribed elastic properties for a fixed amount of material in the base cell. The behavior of both mechanisms and NPR materials is analyzed by discretizing the design domain by four-node quadrilateral

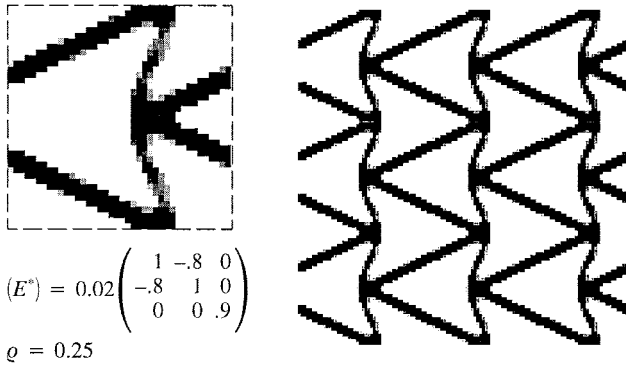


Fig. 3. Material with Poisson's ratio  $-0.8$  obtained from a ground structure with 40 by 40 elements and vertical symmetry enforcement.

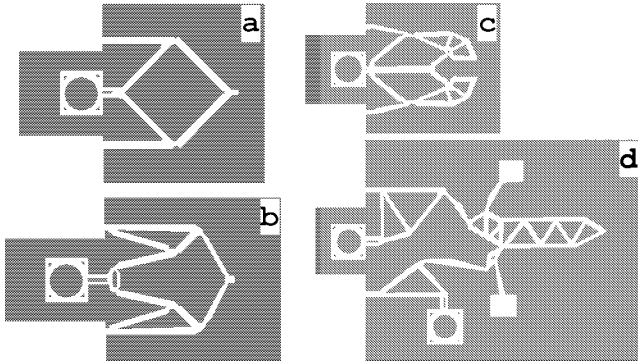


Fig. 4. Four postprocessed micromechanisms: (a) a 1:1 inverter, (b) a 1:4 inverter, (c) a gripper, and (d) a positioner. These designs are now ready to be transferred to the laser micromachining setup.

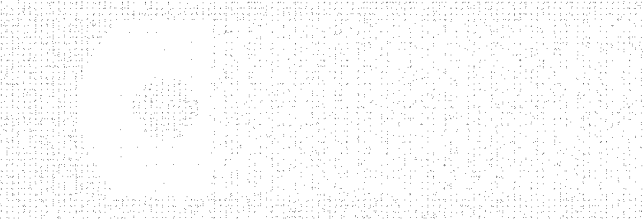


Fig. 5. Interpretation of one of the NPR material designs.

finite elements and solving the finite-element problems for several loading cases. The design variables are given as the density of material in each finite element. As in the previous section, the optimization problems are solved using the SLP method.

#### A. Computational Method

The behavior of a linear elastic material follows the generalized Hooke's law

$$\sigma_{ij} = E_{ijkl} \varepsilon_{kl} \quad (2)$$

where  $E_{ijkl}$  is the elasticity tensor and  $\sigma_{ij}$  and  $\varepsilon_{ij}$  are the stress and strain tensors. By distributing a prescribed amount of material within the design domain (the base cell), we can design a porous and periodic structure with the prescribed elasticity tensor  $E_{ijkl}^*$ , assuming plane stress conditions and

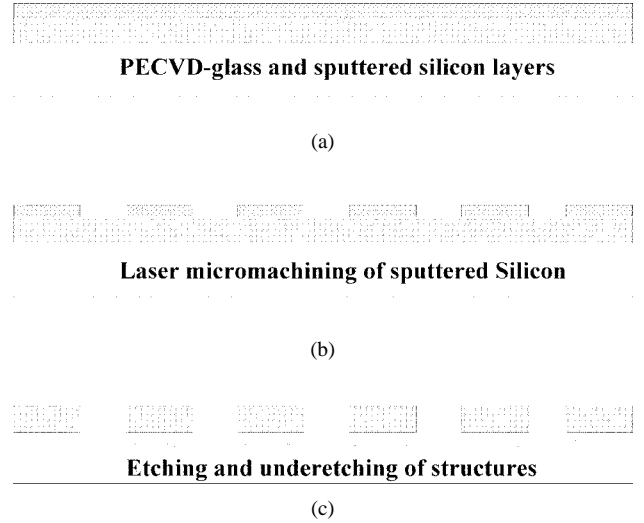


Fig. 6. Steps in the process sequence after (a) deposition of  $6\text{-}\mu\text{m}$  PECVD glass and  $2\text{-}\mu\text{m}$  silicon, (b) laser micromachining of a prototype mask, and (c) two-step RIE process: anisotropic glass etch followed by an isotropic silicon etch.

with prescribed density  $\rho_{\text{cell}}^*$ . Again, the optimization problem is formulated as a least-squares problem

$$\begin{aligned} &\text{Minimize} \quad \Phi = (E_{ijkl}^H - E_{ijkl}^*)^2 \\ &\text{subject to} \quad \sum_{e=1}^N \rho^e v^e \leq \rho_{\text{cell}}^* \\ &\text{and} \quad 0 < \rho_{\min} \leq \rho^e \leq 1, \quad e = 1, \dots, N \end{aligned} \quad (3)$$

where, as before,  $N$  is the number of finite elements or design variables,  $\rho^e$  is the density of material in element  $e$  (design variable  $e$ ),  $\rho_{\min}$  is the lower side constraint on the design variables (for computational reasons), and  $v^e$  is the volume of element  $e$ .  $E_{ijkl}^H$  denotes the homogenized or averaged elasticity tensor for the inhomogeneous material, which can be found using the standard homogenization method (e.g., Bourgat [19]). The homogenization method implies the solving of a finite-element problem with three load cases, namely, a horizontal pull, vertical pull, and shear pulling case, just as one would do to test a real material.

#### B. NPR Material Design Examples

Design of an NPR material was done by specifying the elastic properties of a material with Poisson's ratio  $-0.8$  and solving the optimization problem (3) for a quadratic base cell discretized by 1600 quadrilateral finite elements, each representing one design variable. The resulting topology is seen in Fig. 3 (left). The base cell is repeated in Fig. 3 (right), where the mechanism is seen more clearly. When the material is compressed horizontally, the triangles will collapse and result in a vertical contraction, which is the characteristic behavior of an NPR material.

### IV. FABRICATION OF MICROSTRUCTURES

The achieved designs for compliant micromechanisms and NPR materials were fabricated using silicon surface micromachining. The fabrication method employs a direct writing

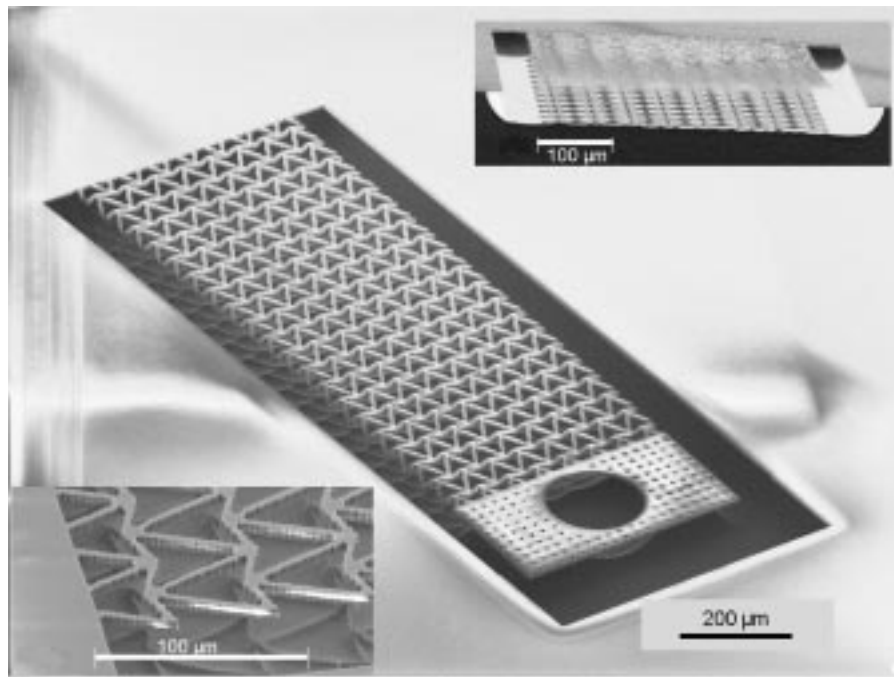


Fig. 7. NPR material testing bar composed of 20 by 8 unit cells. The handle is seen in the front. Upper right: view of the cantilever in the axial direction, after cleaving. The pattern of the beam is also present at the bottom of the recess. Lower left: closeup of the NPR material. The roughness of the side walls is due to the finite resolution of the laser micromachining.

approach, using laser micromachining of a silicon mask layer sputtered on top of a deposited glass layer. To manufacture the mask for the mechanisms and NPR materials, we need to create an input file containing the patterns for the laser micromachining. The mask is a “negative” of the structure, as seen in Fig. 4, since the dark areas denote the areas to be removed by the laser. The numerically produced topologies should be slightly postprocessed by the operator, however, they are easily interpreted as frame structures. The only points of caution are the grey regions, where the topologies are not clearly defined. Currently, the grey areas are manually interpreted, but we are working on improving the method such that interpretation can be done automatically using a density–contour-based algorithm. The thickness of the narrow regions (hinges) has a great influence on the overall behavior and maximum stress in the mechanism. The optimal thickness and shapes of the hinges are currently being investigated using detailed finite-element analysis. In the present work, the thickness and shape of the hinges are decided by the perception of the engineer. Some of the postprocessed mechanisms are shown in Fig. 4.

To be able to mechanically test the NPR material, the base cell is repeated eight and twenty times in the two directions. The resulting bar is clamped at one end and equipped with a handle at the other end, as seen in Fig. 5.

The structures were realized in an isotropic 6-m-thick PECVD glass. This type of material as device layer enables us to make thick films ( $>5 \mu\text{m}$ ) without grain boundaries and with very low stress and isotropic elastic properties. The PECVD glass was deposited on a 4-in,  $\langle 100 \rangle$  silicon wafer and, subsequently, thermally annealed at  $800^\circ\text{C}$  in  $\text{N}_2$  for 1.7 h to bring the compressive stress in the glass close to zero.

The usage of a PECVD glass enables us to employ a simple two-step reactive ion etching (RIE) process to make suspended structures. A  $2\text{-}\mu\text{m}$ -thick silicon was sputtered on top of the glass layer to be used as a masking layer [Fig. 6(a)]. The mechanism designs were etched into the sputtered silicon by direct etching with a laser micromachining system [Fig. 6(b)] [6], [20]. This method of rapid prototyping made it possible to test a large amount of device designs as they were completed. The spot shape of the  $1\text{-}\mu\text{m}$  laser beam results in a roughness of the side walls as it is seen on the side of the structure in Fig. 7 (lower left). The structures were etched into the glass utilizing a two-step RIE process that includes a  $6\text{-}\mu\text{m}$  anisotropic glass etch in  $\text{CF}_4/\text{CHF}_3$  and a  $20\text{-}\mu\text{m}$  isotropic silicon etch in  $\text{SF}_6$  at 120 mTorr.

In Fig. 7, the final result of a suspended NPR material beam can be seen. In the upper right of Fig. 7, the cross section of the beam shows the isotropy of the RIE etch; the selectivity is approximately 1:2. Fig. 8 shows three compliant mechanism prototypes.

## V. EXPERIMENTAL RESULTS

The samples with the micromechanisms were placed on a chuck with a vacuum fixture (Fig. 9). To operate the structures, a probe on a vertically adjustable arm was placed on an  $x$ - $y$  stage. The stage was manually operated, and the movements were measured on a scale with  $0.5\text{-}\mu\text{m}$  resolution. The structures can be monitored on a screen using a video camera, and the response of the mechanisms was recorded on a video tape for subsequent evaluation.

For the NPR materials, the sideways extensions were determined by adding the two sideways displacements of the two

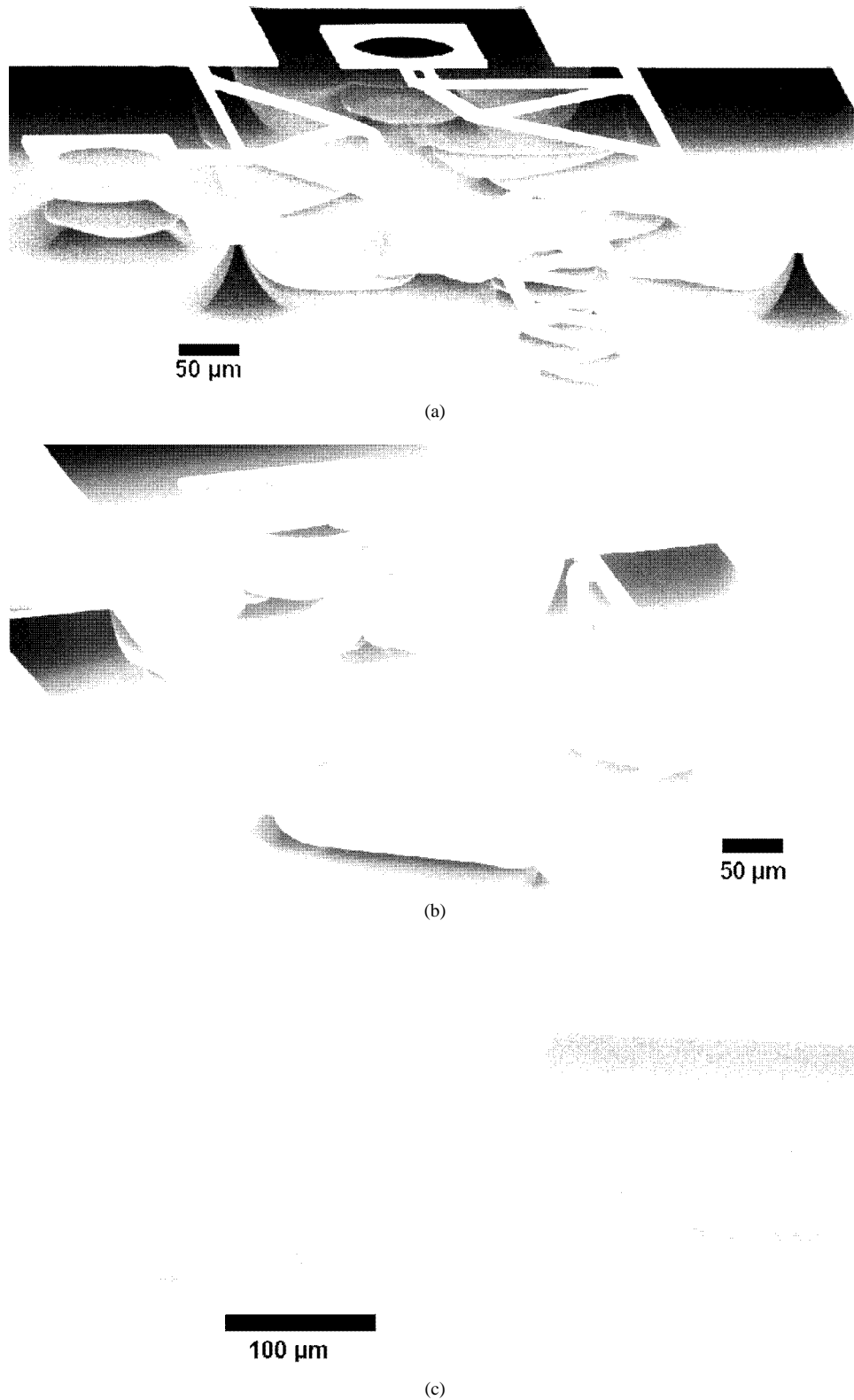


Fig. 8. Compliant micromechanisms: (a) a positioner mechanism, (b) 4:1 inverter mechanism, and (c) gripper mechanism.

sides of the cantilever. The Poisson's ratio can be found from

$$\nu = \frac{-\Delta b/b}{\Delta l/l} \quad (4)$$

where  $\Delta b$  is the sideways extension,  $\Delta l$  is the axial elongation,  $b$  is the width, and  $l$  is the length of the beam. In the practical test, the NPR materials designed for a Poisson's ratio of  $-0.8$

were measured to have an NPR of  $0.92 \pm 13\%$  up to a 1.6% elongation [see Fig. 10(a)].

Output displacements were determined using a ruler on the screen after calibration. The accuracy is determined by the resolution, which amounts to  $1 \mu\text{m}$ . The graph in Fig. 10(b) presents the response of the 1:1 and 1:4 displacement invert-

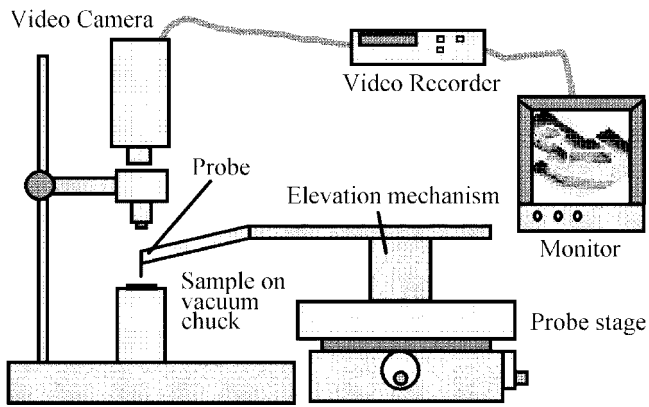


Fig. 9. Test setup. The samples are placed on a chuck, and the mechanisms are tested by a probe on a stage. The movements are recorded. The experiments are evaluated using a monitor.

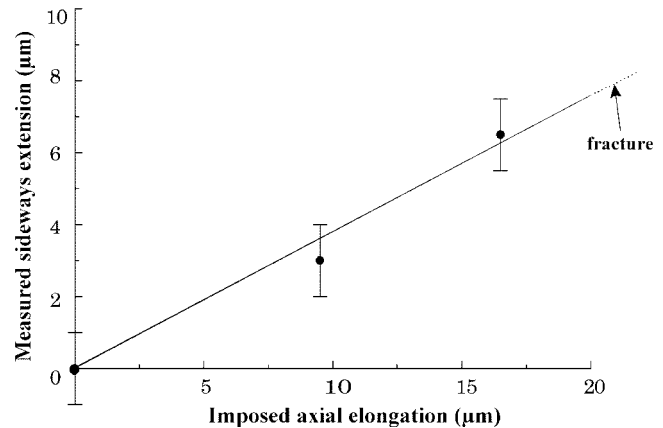
ers. They both show good linearity until the moment where buckling appears. In the linear regions, the response of the 1:1 and 1:4 displacement inverters are  $1:1 \pm 10\%$  and  $1:3.6 \pm 10\%$ , respectively. Eventually, the structures fracture.

#### A. Discussion

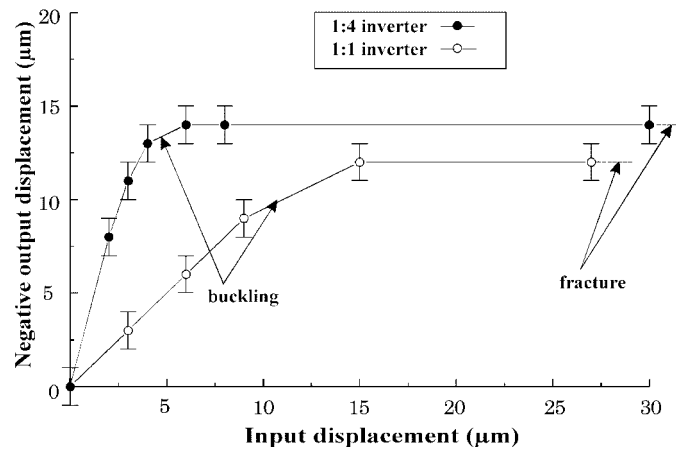
Experience shows that one should be careful with 2-D calculations when the width of the interconnections becomes larger than the thickness of the structure layer. To reach better results, the structures should be fabricated using thicker layers, for instance, by using electroplated materials. Requirements could also be reached by scaling down the mechanisms, but this would require higher resolution of the fabrication methods. Elongations larger than 2% could not be reached because the structures' fracture due to stress concentrations in the fragile glass material. More enduring structures would be obtained with thicker films or by using more elastic and less brittle materials, such as polymers or electroplated copper or nickel, which require alternative fabrication techniques. Nonlinearities such as those due to buckling could be avoided by increasing the widths of buckling-prone elements in the structure.

## VI. CONCLUSION

Compliant micromechanisms have the advantage that they can be built in one piece with very few fabrication steps. Compliant micromechanisms and materials with NPR have been designed using a computational design tool to generate topology-optimized structures. The method allows the user to specify the MA's or GA's of the compliant mechanisms, and the resulting topologies are easily interpreted by the engineer. The generated mechanical structures and NPR materials are fabricated in PECVD glass by etching a pattern into a masking layer with a laser micromachining setup and, subsequently, etching and underetching the oxinitride in two RIE processes. Structures for force or displacement amplifiers, attenuators, and inverters and materials with NPR can easily be designed and fabricated. Design, fabrication, and characterization can be done within one/two days, leading to fast prototyping.



(a)



(b)

Fig. 10. (a) Response of an NPR material. Measured sideways extension versus imposed axial elongation. The resulting NPR measured was  $0.92 \pm 13\%$ . (b) Measured response of 1:1 and 1:4 displacement inverters. The linear displacement transformation holds until buckling appears, and, eventually, the structures fracture. The resulting linear displacement inversions measured were  $1:1 \pm 10\%$  and  $1:3.6 \pm 10\%$ , respectively.

## ACKNOWLEDGMENT

The authors would like to thank M. Müllenborn for his assistance with the laser micromachining, T. Storgaard-Larsen and L. S. Johansen for useful information on processing, and the laboratory staff for assistance with processing in the cleanroom.

## REFERENCES

- [1] G. Thornell, M. Bexell, J.-Å. Schweitz, and S. Johansson, "The design and fabrication of a gripping tool for micromanipulation," in *Dig. Tech. Papers Transducers '95*, nos. 1-3, pp. 388-391.
- [2] J. F. L. Goosen and R. F. Wolfenbuttel, "Object positioning using a surface micromachined distributed system," in *Dig. Tech. Papers Transducers '95*, pp. 396-399.
- [3] P.-F. Indermuehle, C. Linder, J. Brugger, V. P. Jaecklin, and N. F. de Rooij, "Design and fabrication of an overhanging *xy*-microactuator with integrated tip for scanning surface profiling," *Sens. Actuators A*, vol. 43, pp. 346-350, 1994.
- [4] C. G. Keller and R. T. Howe, "Nickel-filled hexsil thermally actuated tweezers," in *Dig. Tech. Papers Transducers '95*, pp. 376-379.
- [5] A. G. Erdman and G. N. Sandor, *Mechanism Design, Analysis and Synthesis*, vol. 1. London, U.K.: Prentice-Hall, 1991.
- [6] M. Müllenborn, H. Dirac, J. W. Petersen, and S. Bouwstra, "Fast 3D laser micromachining of silicon for micromechanical and microfluidic applications," in *Dig. Tech. Papers Transducers '95*, pp. 166-169.

- [7] A.-L. Tiensuu, M. Bexell, J.-Å. Schweitz, L. Smith, and S. Johansson, "Assembling three-dimensional microstructures using gold-silicon eutectic bonding," *Sens. Actuators A*, vol. 45, no. 3, pp. 227–236, 1994.
- [8] W. Riethmüller and W. Benecke, "Thermally excited silicon microactuators," *IEEE Trans. Electron Devices*, vol. 35, no. 6, p. 758, 1988.
- [9] L. L. Howell and A. Midha, "A method for the design of compliant mechanisms with small length flexural pivots," *J. Mech. Design*, vol. 116, no. 1, pp. 280–290, Mar. 1994.
- [10] G. K. Ananthasuresh, S. Kota, and Y. Gianchandani, "A methodical approach to the design of compliant micromechanisms," in *Solid-State Sensor and Actuator Workshop*, June 1994, pp. 189–192.
- [11] O. Sigmund, "Some inverse problems in topology design of materials and mechanisms," in *Proc. IUTAM Symp. on Optimization of Mechanical Systems*, Stuttgart, Germany, Mar. 1995, pp. 277–284.
- [12] M. P. Bendse and N. Kikuchi, "Generating optimal topologies in structural design using a homogenization method," *Comp. Meth. Appl. Mech. Eng.*, vol. 71 pp. 197–224, 1988.
- [13] M. P. Bendsøe, *Methods for the Optimization of Structural Topology, Shape and Material*. Berlin, Germany: Springer-Verlag, 1995.
- [14] M. Avellanada and P. J. Swart, "Calculating the performance of 1–3 piezo composites for hydrophone applications: An effective medium approach," to be published.
- [15] R. F. Almgren, "An isotropic three-dimensional structure with Poisson's ratio =  $-1$ ," *J. Elasticity*, vol. 15, no. 4, pp. 427–430, 1985.
- [16] R. Lakes, "Foam structures with negative Poisson's ratio," *Science*, vol. 235, p. 1038, Feb. 1987.
- [17] O. Sigmund, "Materials with prescribed constitutive parameters: An inverse homogenization problem," *Int. J. Solids Struct.*, vol. 31, no. 17, pp. 2313–2329, 1994.
- [18] O. Sigmund, "Design of material structures using topology optimization," Ph.D. dissertation, Danish Center Appl. Math. Mech., Tech. Univ. Denmark, Lyngby, Denmark, 1994.
- [19] J. F. Bourgat, "Numerical experiments of the homogenization method for operators with periodic coefficients," in *Lecture Notes in Mathematics* 704. Berlin, Germany, Springer-Verlag, 1977, pp. 330–356.
- [20] M. Müllenborn, M. Heschel, U. D. Larsen, H. Dirac, and S. Bouwstra, "Laser direct etching of silicon on oxide for rapid prototyping," *J. Micromech. Microeng.*, vol. 6, no. 1, pp. 49–51, 1996.



**Ole Sigmund** received the M.S. and Ph.D. degrees from the Technical University of Denmark, Lyngby, in 1991 and 1994, respectively.

He was a Research Assistant at the University of Essen, Germany, and a Post-Graduate Fellow at Princeton Materials Institute, Princeton University, Princeton, NJ. He is currently an Assistant Research Professor at the Department of Solid Mechanics at the Technical University of Denmark. His research concentrates on applications of topology optimization methods to material design, rigid and compliant

mechanism design, and smart materials design.



**Siebe Bouwstra** received the Ph.D. degree in 1990 from the University of Twente, Enschede, the Netherlands.

In November 1992, he was appointed Associate Professor at Mikroelektronik Centret at the Technical University of Denmark, Lyngby, where he is responsible for building the micromechanics program.

Dr. Bouwstra was awarded a Research Fellowship from the Royal Dutch Academy of Science, with which he developed novel approaches for silicon resonators in collaboration with the University of Michigan, Ann Arbor.



**Ulrik Darling Larsen** received the M.S. degree in 1994 from the Technical University of Denmark, Lyngby. He is currently working towards the Ph.D. degree in microliquid handling systems at the Technical University of Denmark.

He is a Research Assistant at Mikroelektronik Centret, Lyngby, fabricating compliant micromechanisms and, subsequently, microfluidics.